

AN IONIZATION CONE IN THE DWARF STARBURST GALAXY NGC 5253¹

JORDAN ZASTROW², M.S. OEY², SYLVAIN VEILLEUX³, MICHAEL McDONALD⁴, CRYSTAL L. MARTIN⁵

*** Accepted to ApJ Letters 28 Sept 2011***

ABSTRACT

There are few observational constraints on how the escape of ionizing photons from starburst galaxies depends on galactic parameters. Here, we report on the first major detection of an ionization cone in NGC 5253, a nearby starburst galaxy. This high-excitation feature is identified by mapping the emission-line ratios in the galaxy using [S III] λ 9069, [S II] λ 6716, and H α narrow-band images from the Maryland-Magellan Tunable Filter at Las Campanas Observatory. The ionization cone appears optically thin, which is suggestive of the escape of ionizing photons. The cone morphology is narrow with an estimated solid angle covering just 3% of 4π steradians, and the young, massive clusters of the nuclear starburst can easily generate the radiation required to ionize the cone. Although less likely, we cannot rule out the possibility of an obscured AGN source. An echelle spectrum along the minor axis shows complex kinematics that are consistent with outflow activity. The narrow morphology of the ionization cone supports the scenario that an orientation bias contributes to the difficulty in detecting Lyman continuum emission from starbursts and Lyman break galaxies.

Subject headings: galaxies: evolution — galaxies: individual (NGC 5253) — galaxies: ISM — galaxies: starburst — ISM: jets and outflows — radiative transfer

1. INTRODUCTION

The fate of ionizing photons in starburst galaxies is a critical issue for our understanding of cosmic reionization. Early-epoch star-forming galaxies are the most likely candidate source for the required ionizing radiation (e.g., Madau et al. 1999; Fan et al. 2001). However, quantifying the escape fraction of ionizing radiation (f_{esc}) has proven to be challenging.

Generally, the interstellar medium (ISM) is optically thick to Lyman continuum. As discussed by Heckman et al. (2011), the average hydrogen column density in galaxies ranges from a factor 10^4 to 10^7 times higher than the column that produces unity optical depth in the Lyman continuum. Thus, f_{esc} will be dependent on the morphology of the ISM. For example, models have shown that a clumpy ISM yields a higher f_{esc} than a smoothly varying medium (e.g., Ciardi et al. 2002; Fernandez & Shull 2011). For ionizing radiation to escape, low density paths out of the galaxy must be created. In starburst galaxies, the mechanical feedback from massive stars creates low density bubbles in the ISM, which can then go on to break out of the galactic disk, facilitating the escape of radiation (e.g., Mac Low & McCray 1988; Clarke & Oey 2002). However, the influence of feedback on f_{esc} is not straightforward. Simulations show that the very shells and bubbles that generate low-density holes in the ISM can initially trap ionizing photons before breakout, which will affect f_{esc} (Fujita et al. 2003; Dove et al.

2000).

Understanding this problem is complicated by the small number of galaxies detected with significant f_{esc} , despite large effort by the community to measure it both locally and at high redshift. Direct detection of excess Lyman continuum has been found in a subset of $z \sim 3$ Lyman-break galaxies (e.g. Steidel et al. 2001). However, the fraction of galaxies with high f_{esc} is low, on the order of 10% (e.g., Iwata et al. 2009; Shapley et al. 2006). For local starbursts, the detection rate drops, and most studies obtain upper limits to f_{esc} of a few percent (e.g., Leitherer et al. 1995; Heckman et al. 2001; Grimes et al. 2009; Siana et al. 2010).

One possible explanation for the low detection rate is an orientation bias. In the paradigm outlined above, feedback processes will create passageways perpendicular to the galaxy plane. It follows that ionizing photons will preferentially escape in that direction with an opening angle dependent on galactic conditions (Dove et al. 2000; Gnedin et al. 2008; Fernandez & Shull 2011). Direct measurements of f_{esc} will thus depend on the orientation of the galaxy to our line-of-sight. This model is conducive to the formation of photoionized ionization cones. While photoionized emission has been observed in outflows near starburst nuclei (e.g., Sharp & Bland-Hawthorn 2010; Shopbell & Bland-Hawthorn 1998), clear evidence for ionization cones extending well into the galaxy halo has not yet been observed. Here, we report a new detection of such an ionization cone in a starburst galaxy, NGC 5253. Its narrow opening angle suggests that orientation may play an important role in the detectability of escaping Lyman continuum radiation.

2. OBSERVATIONS

NGC 5253 is a nearby, dwarf galaxy undergoing intense, centrally concentrated star formation. The most recent episode of star formation produced massive super

¹ This paper includes data gathered with the 6.5 meter Magellan Telescopes located at Las Campanas Observatory, Chile.

² Department of Astronomy, University of Michigan, 830 Denison Building, 500 Church Street, Ann Arbor, MI, 48109-1042, USA; JZ: jazast@umich.edu

³ Department of Astronomy, University of Maryland, College Park, MD 20742, USA

⁴ Kavli Institute for Astrophysics and Space Research, MIT, Cambridge, MA 02139, USA

⁵ Department of Physics, University of California, Santa Barbara, CA 93106, USA

star clusters with ages of just a few Myr (e.g., Calzetti et al. 1997). At a distance of 3.8 Mpc (Sakai et al. 2004), we are able to resolve structure down to tens of parsecs. NGC 5253 is well studied across many wavelengths, providing much ancillary data to augment this study.

To identify channels where Lyman continuum radiation might escape from the galaxy, we apply the technique of ionization parameter mapping (e.g., Pellegrini et al., in preparation; Pogge 1988). The ionization parameter is a measure of the ionizing radiation energy density relative to the gas density, and it can be mapped by emission-line ratios that probe high- vs low-ionization species. Regions that are optically thick to ionizing radiation show a low-ionization boundary between the highly ionized regions close to the ionizing source and the neutral environment; whereas optically thin regions maintain high excitation throughout. For this study, we use [S III] $\lambda 9069$ and [S II] $\lambda 6716$ to map the high- and low-ionization species, respectively.

We obtained narrow-band images of NGC 5253 on the nights of 2009 July 9–11 using the Maryland-Magellan Tunable Filter (MMTF; Veilleux et al. 2010). The bandpasses include $H\alpha$ and narrow-band continuum imaging observed at the redshift of NGC 5253. They are given in Table 1, together with their exposure times. MMTF uses a low-order Fabry-Perot etalon and is mounted on the imaging spectrograph, IMACS, of the Magellan Baade telescope at Las Campanas Observatory. The IMACS f/2 camera has an $8K \times 8K$ Mosaic CCD with a pixel scale of $0.2''$ per pixel. For these observations, MMTF was used at low etalon spacings to provide a monochromatic field of view of $11.5'$. We additionally obtained a long-slit spectrum of NGC 5253. The seeing conditions ranged from $0.5''$ – $0.7''$ for the [S II] and [S III] images and $1.5''$ – $2''$ for $H\alpha$.

The bias subtraction, flat-fielding, and sky subtraction are accomplished using version 1.4 of the MMTF data reduction pipeline,⁶ described in Veilleux et al. (2010). The $H\alpha$ -continuum image is first flux calibrated using photometry from standard star observations. Then, the long slit spectrum is corrected for instrument response using standard star spectra, and flux calibrated using the flux-calibrated, $H\alpha$ -continuum image. Finally, the other emission-line images are normalized to the emission measured across each bandpass in the flux-calibrated, long slit spectrum. Systematic errors for the flux calibration are about a factor of two. The images are registered and rescaled using standard IRAF⁷ tasks, then continuum subtracted. Galactic extinction is corrected assuming $E(B-V) = 0.0475$ across the field (Burstein & Heiles 1982) and the extinction law from Cardelli et al. (1989). The internal extinction is known to be variable throughout the galaxy (Calzetti et al. 1997; Caldwell & Phillips 1989; Cresci et al. 2005), and its effects are discussed in § 3.1.

A three-color composite of our data is presented in Figure 1, along with the continuum-subtracted, emission-line images. Sky background and noise properties of the images are measured using the median and standard de-

viation in the flux of fifteen $20'' \times 20''$ boxes around the galaxy. In $H\alpha$, we have a 3σ confidence detection limit of 4.1×10^{-18} erg s $^{-1}$ cm $^{-2}$. The ionized gas in the galaxy has a roughly spherical distribution around the nucleus, with networks of loops and filaments particularly noticeable to the south and northwest (e.g., Marlowe et al. 1995).

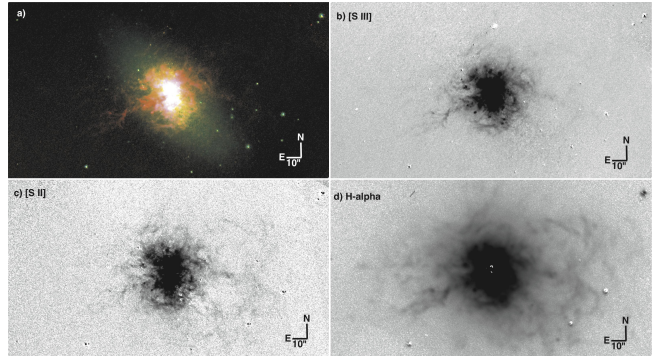


Figure 1. *a)* Composite image of NGC 5253. Red, blue and green correspond to [S III], [S II], and continuum at $\lambda 6680$, respectively. Ionization cone extends ESE from the nuclear starburst. Panels *b*, *c*, and *d* show individual continuum-subtracted, [S III], [S II], and $H\alpha$, respectively. At a distance of 3.8 Mpc, $10'' = 180$ pc.

3. IONIZATION CONE IN NGC 5253

3.1. Morphology and Excitation of the Ionization Cone

NGC 5253 shows a stunning detection of an ionization cone in a starburst galaxy. In Figure 1, the ionization cone stands out beautifully, extending ESE along the minor axis. In the ratio map, Figure 2, the ionization cone is identified by its high excitation relative to the rest of the galaxy. This high excitation has also been observed in [O III]/[S II] (Calzetti et al. 1999). It has an opening angle $< 40^\circ$ with a narrow appearance at large radii. As the distance from the galaxy increases, the morphology of the cone becomes filamentary. While the cone appears to be one-sided, we note that extended [S III] emission to the northwest may suggest a bi-cone (Figure 1).

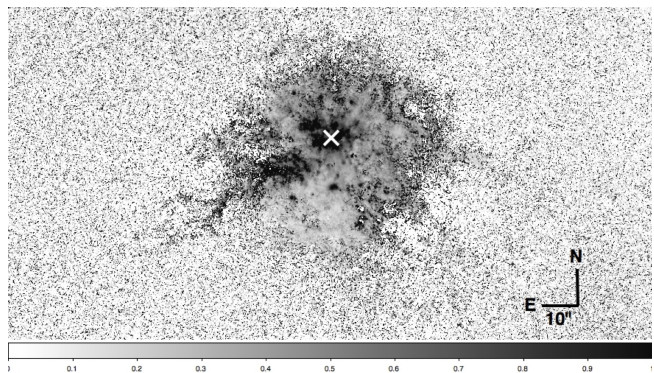


Figure 2. [S III]/[S II] ratio map for NGC 5253. Dark indicates high values of [S III]/[S II].

The changes in ionization parameter as a function of radius are shown more quantitatively in Figure 3. These plots are generated using 3×3 binning of the continuum-subtracted images, and a 3σ detection cut-off in all three

⁶ <http://www.astro.umd.edu/~veilleux/mmtf/datared.html>

⁷ IRAF is distributed by NOAO, which is operated by AURA, Inc., under cooperative agreement with the National Science Foundation.

Table 1
Observations

Emission line	Wavelength (Å)	Effective Bandpass (Å)	Exp. Time	Flux ^a (10^{-13} erg s ⁻¹ cm ⁻²)
[S III]	9081	27.0	5 × 1200 s	0.39
continuum	9180	27.0	5 × 1200 s	...
[S II]	6726	16.2	5 × 1200 s	0.59
continuum	6680	16.2	5 × 1200 s	...
H α	6572	18.5	3 × 1200 s	12.9
continuum	6680	18.5	3 × 1200 s	...

^a Continuum-subtracted flux measured in the ionization cone using the DS9 ftools module.

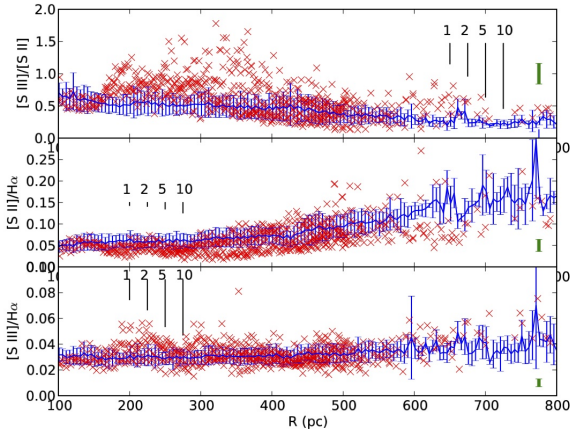


Figure 3. Emission-line ratios vs. galactocentric radius. Red represents ionization cone emission. Blue line is the mean galactic value in radial bins, with bars noting one standard deviation. Representative measurement error is shown by the green error bar. The black lines indicate the effect of different levels of extinction ($A_V = 1, 2, 5, 10$). Top, middle, and bottom panels show $[S\ III]/[S\ II]$, $[S\ II]/H\alpha$, and $[S\ III]/H\alpha$, respectively.

emission lines. The ionization cone, shown in red, is defined as the region between P.A. = 102° – 140° using $\alpha = 13^h39^m55^s.7$, $\delta = -31^\circ38'24''$ (J2000) as the apex. This point, marked by the cross in Figure 2, is the location of a likely source for the ionizing radiation, as discussed below. For comparison, the blue line is representative of the rest of the galaxy.

The top panel of Figure 3 clearly shows a strong excess in the $[S\ III]/[S\ II]$ ratio for the ionization cone at lower galactocentric radii R , and a clear excess that continues to $R \sim 600 - 700$ pc. The middle and lower panels show that this excess cannot be explained solely by the well-known increasing gradient in $[S\ II]/H\alpha$ that is found in the diffuse, ionized gas of star-forming galaxies (e.g., Rand 1998; Haffner et al. 1999). Furthermore, Figure 1 shows that the primary star-forming region extends only to ~ 500 pc, whereas photoionized material associated with the cone clearly extends beyond. This strongly suggests that there is not enough gas in the outer halo to absorb all the ionizing photons, and that they therefore may escape the galaxy.

As noted above, the extinction throughout the starburst is variable (Cresci et al. 2005), and might enhance the observed $[S\ III]/[S\ II]$ ratio relative to the intrinsic one. In particular, a dust lane with associated CO along the minor axis is coincident with the location of the cone (Calzetti et al. 1997; Caldwell & Phillips 1989; Meier

et al. 2002). However, Figure 3 shows that we need $A_V \sim 3 - 10$ mag to explain the observed $[S\ III]/[S\ II]$ ratios entirely by the dust lane, which is much more than its observed extinction ($A_V \sim 2.2$ mag, Calzetti et al. 1997). If there were that much extinction, we would expect a much lower flux along the cone, which is not seen in the emission-line images in Figure 1. Additionally, the $[S\ II]/H\alpha$ ratio observed in the cone cannot be explained by extinction. We also note that the highest extinction will likely be strongest at the smallest R .

Another possible effect is a bias in our observed $[S\ III]/[S\ II]$ ratio caused by strong variations in electron density. This affects the $[S\ II]\lambda 6716/\lambda 6731$ ratio, so that our observed $\lambda 6716$ may underestimate the total $[S\ II]$ at high density. This error again will be largest at smaller radii where densities are larger, and leads to difference of $\sim 25\%$ between a density of 10^2 and 10^3 cm⁻³. In our long-slit spectrum, $[S\ II]\lambda\lambda 6716/6731$ ratio ranges from 1.4 to 1.0, which correspond to densities of $\lesssim 100$ cm⁻³ and ~ 500 cm⁻³, respectively. Since this is a smaller variation than between 10^2 and 10^3 cm⁻³, the error on our observed $[S\ II]$ due to density variations is likely much less than 25%.

The measured emission-line fluxes in the ionization cone (Table 1) can set limits on the ionizing source. The H α flux corresponds to an H α luminosity $L(H\alpha) = 2.2(\pm 1.1) \times 10^{39}$ erg s⁻¹. This is $\sim 6\%$ the total $L(H\alpha)$ in the galaxy (Marlowe et al. 1995, corrected for distance), from which we obtain a lower limit of $\log(Q_0) \geq 51.19$ on the rate of ionizing photons, Q_0 (s⁻¹), needed to explain the observed emission. An O7 star with the $\sim 0.2 Z_\odot$ metallicity of NGC 5253 (Walsh & Roy 1989) has $\log(Q_0) = 49.0$ (Smith et al. 2002). This implies that radiation equivalent to that produced by $\gtrsim 160 \pm 80$ O7 stars is needed to ionize the gas. This is a lower limit for the radiation escaping the nuclear starburst, since the flux will be affected by internal extinction and f_{esc} .

NGC 5253 is host to many young clusters that could be the source for the ionizing radiation illuminating the cone. Two likely candidates are NGC 5253-5 (Calzetti et al. 1997) and the ionizing cluster of the radio supernebula (Beck et al. 1996; Turner et al. 2000; Gorjian et al. 2001). The location of these objects, separated by just a few arcseconds on the sky (Alonso-Herrero et al. 2004), is noted by the cross in Figure 2. Both clusters are very young and very massive (Turner et al. 2000; Calzetti et al. 1997; Alonso-Herrero et al. 2004). In fact, the radio supernebula may be gravitationally confined (Turner et al. 2003). The 20 pc region around the radio supernebula hosts an ionizing population ~ 7000 O7 stars, with some uncertainty due to the high extinction

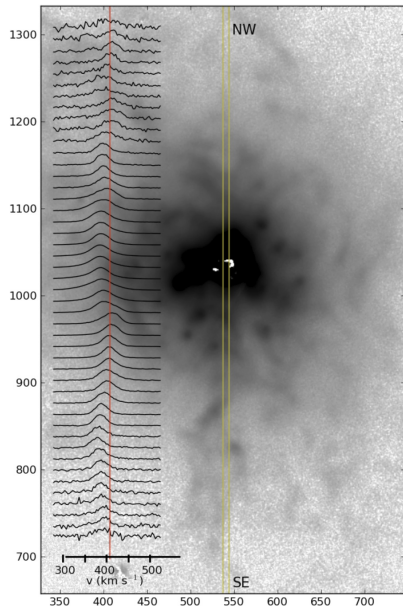


Figure 4. NGC 5253 $H\alpha$ image, minor axis oriented along the y -axis. $H\alpha$ echelle profiles are overlaid to the left. The profiles are normalized to a peak of one and the spacing between each profile is $2.''6$. The red line denotes the v_{sys} for NGC 5253, reported to be $407 \pm 3 \text{ km s}^{-1}$ (Koribalski *et al.* 2004). The slit position is marked in yellow.

towards this cluster (Turner & Beck 2004). Thus, the clusters in NGC 5253 easily generate enough ionizing flux to explain the ionization cone.

3.2. Kinematics

The HI kinematics in NGC 5253 show only small scale rotation about the minor axis (Kobulnicky & Skillman 2008), making it unlikely that NGC 5253 is rotationally supported (Caldwell & Phillips 1989). In Figure 4, the line profiles from an $H\alpha$ echellegram (Slit 3, Martin & Kennicutt 1995) are overlaid on the $H\alpha$ image of NGC 5253. The velocity shows significant variation with position, and a maximum projected velocity difference $\Delta v \sim 30 \text{ km s}^{-1}$ relative to systemic.

An expanding wind might explain the kinematics. In this scenario, we expect the velocity to increase with distance from the galaxy, since the wind is expanding into the lower density gas of the halo. To the southeast, we do see an increase in velocity with galactocentric distance. However, it reaches a maximum at $\sim 40''$ from the galaxy center before decreasing towards systemic at larger R . This does not strictly follow what is expected for a free-flowing wind, in which the velocity should continue to increase. Additionally, an expanding wind typically exhibits line splitting, which is not seen in the $H\alpha$ profiles (Martin & Kennicutt 1995). Kinematic data from HI observations are suggestive of either inflow or outflow along the minor axis (Kobulnicky & Skillman 2008). Therefore, although not completely straightforward, mechanical feedback might plausibly explain the observed kinematics based on the limited information available.

3.3. Possible AGN

Typically, ionization cones are associated with AGN, which suggests an alternative explanation for the ionization cone in NGC 5253. The morphology of the cone is very narrow. This suggests collimation of the ionizing radiation, as would be expected if there is an AGN present. The radio supernebula is particularly intriguing in this context. Only $\sim 0.''6$ in size, it provides roughly 80% of the galaxy's IR flux at $12\mu\text{m}$ (Gorjian *et al.* 2001). There is some debate about whether a young super star cluster or AGN is the ionizing source of this nebula. Its radio continuum has a flat slope, consistent with thermal emission (Beck *et al.* 1996; Turner *et al.* 1998, 2000), but which does not rule out an AGN component (Turner *et al.* 1998). However, the observed spectral lines are also narrower than would be expected from an AGN (Beck *et al.* 1996). Additionally, X-ray observations of NGC 5253 show that the point sources and diffuse emission are consistent with star formation and shocks (Ott *et al.* 2005; Summers *et al.* 2004; Martin & Kennicutt 1995). Therefore, while we cannot rule out an AGN in NGC 5253, there are challenges facing that interpretation.

If NGC 5253 has an obscured AGN, a precessing jet might explain the gas kinematics. In this case, the velocities on one side of the galaxy should be mirrored exactly on the opposite side. In NGC 5253, the overall sinusoid in velocity to the southeast is roughly reflected to the northwest. Along the ionization cone, the velocity transitions from redshift to blueshift around $\sim 30''$ from the galaxy. To the northwest, the opposite transition, of roughly equal amplitude, is seen at $\sim 28''$. However, the reflection is not perfect; there are points to the northwest where the velocity briefly flips, which are not seen to the southeast. Additionally, the amount of blueshift to the northwest does not match the redshift observed in the southeast. Therefore, while the general kinematics could be explained by a precessing jet, the discrepancies are difficult to reconcile in detail.

4. IMPLICATIONS: ORIENTATION BIAS

Based on our detection of an ionization cone in NGC 5253, we suggest that an orientation bias can explain the difficulty in detecting escaping ionizing radiation in starburst galaxies. We observe evidence that ionizing radiation from NGC 5253 is traveling to large radii, if not escaping the galaxy entirely. Assuming the cone is axisymmetric, the estimated solid angle subtended by the cone is $\sim 3\%$ of 4π steradians, suggesting that the escape process happens over a small solid angle. If we assume isotropic radiation from 7000 O7 stars, as above, we could expect to see ionized-gas emission in this solid angle equivalent to that produced by 210 O7 stars. This is similar to our estimated 160 ± 80 O7 stars needed to generate the observed $H\alpha$ emission in the cone, supporting the physical link between the source and the cone. The narrow morphology suggests that in order to detect Lyman continuum, the line-of-sight to the galaxy must be close to the axis of escape. Thus, the orientation of the galaxy should strongly influence the detectability of Lyman continuum radiation.

We can find further evidence for this scenario in recent observations by Heckman *et al.* (2011). In their study of

11 Lyman-break analog galaxies and 15 local starbursts, including NGC 5253, they found indirect evidence for significant f_{esc} in three of the Lyman-break analogs. Outflow velocities on the order of 10^3 km s^{-1} were found in all the galaxies suggested to have significant f_{esc} . These outflow velocities are so high, that we can interpret it to mean the direction of the outflow must be closely aligned to the lines-of-sight towards the galaxies. Since winds in starburst galaxies are generally coincident with the poles (Veilleux et al. 2005), this suggests that these inferred high f_{esc} are all associated with face-on systems. This fits our explanation that measurements of large f_{esc} are biased towards galaxies whose outflow happens along our line-of-sight.

5. CONCLUSION

The ionization cone in NGC 5253 provides a new perspective to our understanding of the fate of ionizing photons in starburst galaxies. This ionization cone appears optically thin, which is suggestive of the escape of ionizing radiation along the cone. At minimum, ionizing radiation is escaping from the nuclear starburst into the galaxy's halo. We considered both stellar and non-stellar sources for the ionization cone. Assuming a stellar source, the massive clusters in NGC 5253 produce enough ionizing radiation to explain the $\text{H}\alpha$ emission observed. However, the possibility of an obscured AGN has not been ruled out. The $\text{H}\alpha$ kinematics along the cone exhibit a complex morphology, but are consistent with some form of outflow. The data are not straightforward to interpret, but might be explained by an expanding wind or perhaps a precessing jet.

Using the ionization cone of NGC 5253 as an analog for other starburst galaxies, we see that ionizing radiation escapes along the minor axis. Additionally, the solid angle over which this radiation escapes is small, based on the cone morphology. This will constrain the viewing angles from which Lyman continuum radiation can be detected. Thus, the orientation of the galaxy will strongly influence the ability to detect Lyman continuum radiation. NGC 5253 may be the nearest starburst galaxy with a significant f_{esc} , and offers a unique opportunity to study the emission mechanisms in detail.

We kindly thank David Osip for recovering important data from the Magellan Archives, John Glaspey for converting old image formats to current ones, and Eric Pellegrini for useful discussions. We thank the referee for thorough and helpful comments. This work was funded by NSF grants AST-0806476 to MSO and AST-1009583 to SV.

Facilities: Magellan:Baade()

REFERENCES

Alonso-Herrero, A., Takagi, T., Baker, A. J., Rieke, G. H., Rieke, M. J., Imanishi, M., & Scoville, N. Z. 2004, *ApJ*, 612, 222

- Beck, S. C., Turner, J. L., Ho, P. T. P., Lacy, J. H., & Kelly, D. M. 1996, *ApJ*, 457, 610
- Burstein, D., & Heiles, C. 1982, *AJ*, 87, 1165
- Caldwell, N., & Phillips, M. M. 1989, *ApJ*, 338, 789
- Calzetti, D., Meurer, G. R., Bohlin, R. C., Garnett, D. R., Kinney, A. L., Leitherer, C., & Storchi-Bergmann, T. 1997, *AJ*, 114, 1834
- Calzetti, D., Conelice, C. J., Gallagher, III, J. S., & Kinney, A. L. 1999, *AJ*, 118, 797
- Cardelli, J. A., Clayton, G. C., & Mathis, J. S. 1989, *ApJ*, 345, 245
- Ciardi, B., Bianchi, S., & Ferrara, A. 2002, *MNRAS*, 331, 463
- Clarke, C., & Oey, M. S. 2002, *MNRAS*, 337, 1299
- Cresci, G., Vanzi, L., & Sauvage, M. 2005, *A&A*, 433, 447
- Dove, J. B., Shull, J. M., & Ferrara, A. 2000, *ApJ*, 531, 846
- Fan, X., et al. 2001, *AJ*, 122, 2833
- Fernandez, E. R., & Shull, J. M. 2011, *ApJ*, 731, 20
- Fujita, A., Martin, C. L., Mac Low, M., & Abel, T. 2003, *ApJ*, 599, 50
- Gnedin, N. Y., Kravtsov, A. V., & Chen, H. 2008, *ApJ*, 672, 765
- Gorjian, V., Turner, J. L., & Beck, S. C. 2001, *ApJ*, 554, L29
- Grimes, J. P., et al. 2009, *ApJS*, 181, 272
- Haffner, L. M., Reynolds, R. J., & Tuftes, S. L. 1999, *ApJ*, 523, 223
- Heckman, T. M., Sembach, K. R., Meurer, G. R., Leitherer, C., Calzetti, D., & Martin, C. L. 2001, *ApJ*, 558, 56
- Heckman, T. M., et al. 2011, *ApJ*, 730, 5
- Iwata, I., et al. 2009, *ApJ*, 692, 1287
- Kobulnicky, H. A., & Skillman, E. D. 2008, *AJ*, 135, 527
- Koribalski, B. S., et al. 2004, *AJ*, 128, 16
- Leitherer, C., Ferguson, H. C., Heckman, T. M., & Lowenthal, J. D. 1995, *ApJ*, 454, L19+
- Mac Low, M., & McCray, R. 1988, *ApJ*, 324, 776
- Madau, P., Haardt, F., & Rees, M. J. 1999, *ApJ*, 514, 648
- Marlowe, A. T., Heckman, T. M., Wyse, R. F. G., & Schommer, R. 1995, *ApJ*, 438, 563
- Martin, C. L., & Kennicutt, Jr., R. C. 1995, *ApJ*, 447, 171
- Meier, D. S., Turner, J. L., & Beck, S. C. 2002, *AJ*, 124, 877
- Ott, J., Walter, F., & Brinks, E. 2005, *MNRAS*, 358, 1423
- Pogge, R. W. 1988, *ApJ*, 328, 519
- Rand, R. J. 1998, *ApJ*, 501, 137
- Razoumov, A. O., & Sommer-Larsen, J. 2010, *ApJ*, 710, 1239
- Sakai, S., Ferrarese, L., Kennicutt, Jr., R. C., & Saha, A. 2004, *ApJ*, 608, 42
- Shapley, A. E., Steidel, C. C., Pettini, M., Adelberger, K. L., & Erb, D. K. 2006, *ApJ*, 651, 688
- Sharp, R.G., & Bland-Hawthorn, J. 2010, *ApJ*, 711, 818
- Shoppell, P. L., & Bland-Hawthorn, J. 1998, *ApJ*, 493, 129
- Siana, B., et al. 2010, *ApJ*, 723, 241
- Smith, L. J., Norris, R. P. F., & Crowther, P. A. 2002, *MNRAS*, 337, 1309
- Steidel, C. C., Pettini, M., & Adelberger, K. L. 2001, *ApJ*, 546, 665
- Summers, L. K., Stevens, I. R., Strickland, D. K., & Heckman, T. M. 2004, *MNRAS*, 351, 1
- Turner, J. L., & Beck, S. C. 2004, *ApJ*, 602, L85
- Turner, J. L., Beck, S. C., Crosthwaite, L. P., Larkin, J. E., McLean, I. S., & Meier, D. S. 2003, *Nature*, 423, 621
- Turner, J. L., Beck, S. C., & Ho, P. T. P. 2000, *ApJ*, 532, L109
- Turner, J. L., Ho, P. T. P., & Beck, S. C. 1998, *AJ*, 116, 1212
- Veilleux, S., Cecil, G., & Bland-Hawthorn, J. 2005, *ARA&A*, 43, 769
- Veilleux, S., et al. 2010, *AJ*, 139, 145
- Walsh, J. R., & Roy, J. 1989, *MNRAS*, 239, 297
- Wise, J. H., & Cen, R. 2009, *ApJ*, 693, 984
- Yajima, H., Choi, J., & Nagamine, K. 2011, *MNRAS*, 412, 411